

Photometric detection of non-transiting short-period low-mass companions through the beaming, ellipsoidal and reflection effects in *Kepler* and CoRoT lightcurves

S. Faigler and T. Mazeh

*School of Physics and Astronomy, Raymond and Beverly Sackler Faculty of Exact Sciences,
Tel Aviv University, Tel Aviv 69978, Israel*

submitted Feb 21st, 2011

ABSTRACT

We present a simple algorithm, BEER, to search for a combination of the BEaming, Ellipsoidal and the Reflection/heating periodic modulations, induced by short-period *non-transiting* low-mass companions. The beaming effect is due to the increase (decrease) of the brightness of any light source approaching (receding from) the observer. To first order, the beaming and the reflection/heating effects modulate the stellar brightness at the orbital period, with phases separated by a quarter of a period, whereas the ellipsoidal effect is modulated with the orbital first harmonic. The phase and harmonic differences between the three modulations allow the algorithm to search for a combination of the three effects and identify stellar candidates for low-mass companions. The paper presents the algorithm, including an assignment of a likelihood factor to any possible detection, based on the expected ratio of the beaming and ellipsoidal effects, given an order-of-magnitude estimate of the three effects. As predicted by Loeb & Gaudi (2003) and Zucker, Mazeh & Alexander (2007), the *Kepler* and the CoRoT lightcurves are precise enough to allow detection of massive planets and brown-dwarf/low-mass-stellar companions with orbital period up to 10–30 days. To demonstrate the feasibility of the algorithm, we bring two examples of candidates found in the first 33 days of the Q1 *Kepler* lightcurves. Although we used relatively short timespan, the lightcurves were precise enough to enable the detection of periodic effects with amplitudes as small as one part in 10^4 of the stellar flux.

Key words: methods: data analysis — planetary systems: detection — binaries: spectroscopic — brown dwarfs.

1 INTRODUCTION

We present a simple algorithm, BEER, to search for a combination of the BEaming, Ellipsoidal and the Reflection/heating periodic modulations, induced by short-period *non-transiting* low-mass companions, using precise photometric stellar lightcurves. Two of the modulations are well known for many years from the study of close binary stellar systems. These are the ellipsoidal variation (Morris 1985), due to the tidal distortion of each component by the gravity of its companion (see a review by Mazeh 2008), and the reflection/heating variation (referred here as the reflection modulation), induced by the luminosity of each component that falls only on the close side of its companion (e.g., Maxted et al. 2002; Harrison et al. 2003; For et al. 2010; Reed et al. 2010).

A much smaller and less studied photometric modulation is the beaming effect, sometimes called Doppler boosting, induced by the stellar radial motion. This effect causes an increase (decrease) of the brightness of any light source approaching (receding from) the observer (e.g., Rybicki & Lightman 1979). Before the era of space photometry this effect has been noticed only once, by Maxted et al. (2000), who observed KPD 1930+2752, a binary with a very short period, of little longer than 2 hours, and a radial-velocity amplitude of 350 km/s. The beaming effect of that system, which should be on the order of 10^{-3} , was hardly seen in the photometric data.

The beaming effect became relevant only recently, when space photometry, aimed to detect transits of exo-planets, has substantially improved the precision of the produced lightcurves. The CoRoT (Rouan et al. 1998; Baglin et al. 2006; Auvergne et al. 2009) and *Kepler* (Borucki et al. 2010; Koch et al. 2010) missions are producing hundreds of thousands of continuous photometric lightcurves with timespan of tens and hundreds of days, at relative precision level that can get to 10^{-3} – 10^{-4} per measurement, depending on the stellar brightness. It was therefore anticipated that CoRoT and *Kepler* will detect each of the three modulations (e.g., Drake 2003; Loeb & Gaudi 2003; Zucker et al. 2007), for binaries and planets alike.

As predicted, already in the Q1 *Kepler* data, which spanned over only 33 days, van Kerkwijk et al. (2010) detected the ellipsoidal and the beaming effect of two eclipsing binaries, KOI-74 and

KOI-81 (Rowe et al. 2010). Carter et al. (2010) detected the ellipsoidal, beaming and reflection effects in the *Kepler* lightcurve of the eclipsing binary KIC 10657664, and derived the system parameters from the amplitudes of the three effects, determining the system to be comprised of a low-mass, thermally-bloated, hot white dwarf orbiting an A star. The effects were discovered even for brown-dwarf secondaries and planets. Welsh et al. (2010) identified the ellipsoidal effect in the *Kepler* data of HAT-P-7, a system with a known planet of $1.8 M_{\text{Jup}}$ and a period of 2.2 days (Pál et al. 2008). Snellen et al. (2009) detected in CoRoT data the reflection effect of CoRoT-1b. Mazeh & Faigler (2010) detected the ellipsoidal and the beaming effect induced by CoRoT-3b, a $22 M_{\text{Jup}}$ massive-planet/brown-dwarf companion with a period of 4.3 days (Deleuil et al. 2008).

However, space mission data can yield much more. In addition to eclipse events, CoRoT and *Kepler* are producing data that can indicate the binarity of a system based on the evidence coming only from the beaming, ellipsoidal and reflection effects themselves. Loeb & Gaudi (2003) suggested that the beaming effect can be used to detect non-transiting exo-planets, and Zucker et al. (2007) extended this idea to binaries. Loeb & Gaudi (2003) (see also the discussion of Zucker et al. 2007) showed that for relatively long-period orbits, of the order of 10–100 days, the beaming modulation is stronger than the ellipsoidal and the reflection effects, and therefore could be observed without the interference of the other two modulations. However, the beaming modulation by itself might not be enough to render a star a good exo-planet candidate, as the pure sinusoidal modulation could be produced by other effects, stellar modulations in particular (e.g., Aigrain, Favata & Gilmore 2004). The BEER detection algorithm, therefore, searches for stars that show in their space-obtained lightcurves some *combination* of the three modulations, the ellipsoidal and the beaming effects in particular.

The CoRoT mission, and certainly the *Kepler* satellite, have the required precision to reveal the ellipsoidal and even the beaming modulations for massive planets and brown-dwarf/low-mass-stellar companions with short enough orbital periods. This was demonstrated by Mazeh & Faigler (2010) for the aforementioned CoRoT-3b, for which they detected the two modulations with amplitudes of about 60 and 30 ppm (parts per million), respectively.

Searching for an unknown orbital period is more difficult than looking for a modulation with known period and phase. However, the combination of at least two of the modulations, and their relative amplitudes and *phases*, can suggest the presence of a small non-transiting

companion. Like in the transit searches, the candidates found must be followed by radial velocity (RV) observations, in order to confirm the existence of the low-mass companion, and to reject the other possible interpretations of the photometric modulations.

This paper presents the details of the BEER algorithm. Section 2 presents theoretical approximation of the beaming, ellipsoidal and reflection effects, Section 3 explains the details and performance estimate of the algorithm itself, and Section 4 brings two candidates found in the *Kepler* Q1 data, with a companion mass of, up to the sine of the orbital inclination, $\sim 70 M_{\text{Jup}}$. In a separate paper (Faigler, Mazeh et al., in preparation) we present RV observations that confirm the existence of the two companions. Section 5 summarizes our results and argues that the BEER algorithm can discover short-period brown-dwarf companions and even massive planets, given the CoRoT and *Kepler* data accuracy.

2 THEORETICAL APPROXIMATION OF THE THREE EFFECTS

To perform the search for massive planets and brown-dwarf/low-mass-stellar companions we need order-of-magnitude approximations for the three effects. For the BEER algorithm, we use the expressions listed by Mazeh & Faigler (2010) for circular orbits, assuming the companion is much smaller than the primary star, and therefore ignoring its luminosity. The expressions for a $10 M_{\text{Jup}}$ companion become

$$A_{\text{beam}} = \alpha_{\text{beam}} 4 \frac{K_{\text{RV}}}{c} = 27 \alpha_{\text{beam}} \left(\frac{M_*}{M_{\odot}} \right)^{-2/3} \left(\frac{P_{\text{orb}}}{1 \text{ day}} \right)^{-1/3} \left(\frac{m_2 \sin i}{10 M_{\text{Jup}}} \right) \text{ ppm}, \quad (1)$$

$$A_{\text{ellip}} = \alpha_{\text{ellip}} \frac{m_2 \sin i}{M_*} \left(\frac{R_*}{a} \right)^3 \sin i = 128 \alpha_{\text{ellip}} \sin i \left(\frac{R_*}{R_{\odot}} \right)^3 \left(\frac{M_*}{M_{\odot}} \right)^{-2} \left(\frac{P_{\text{orb}}}{1 \text{ day}} \right)^{-2} \left(\frac{m_2 \sin i}{10 M_{\text{Jup}}} \right) \text{ ppm}, \quad (2)$$

$$A_{\text{refl}} = \alpha_{\text{refl}} 0.1 \left(\frac{r_2}{a} \right)^2 \sin i = 57 \alpha_{\text{refl}} \sin i \left(\frac{M_*}{M_{\odot}} \right)^{-2/3} \left(\frac{P_{\text{orb}}}{1 \text{ day}} \right)^{-4/3} \left(\frac{r_2}{R_{\text{Jup}}} \right)^2 \text{ ppm}. \quad (3)$$

In the above expressions, m_2 and r_2 are the companion mass and radius, M_* and R_* are the primary mass and radius, P_{orb} and a are the orbital period and semi-major axis, K_{RV} is the semi-amplitude of the stellar radial-velocity modulation induced by the companion, i is the orbital inclination relative to our line of sight, and c is the speed of light.

The α 's represent order-of-unity coefficients that necessitate more detailed model to evaluate:

- The expression for the beaming effect includes two factors. The $4K_{\text{RV}}/c$ factor represents the beaming effect for bolometric photometric observations, but ignores the Doppler shift photometric effect, which appears when the photometric observations are made in a specific

bandpass, so that some of the stellar light is shifted out of or into the observed bandpass. The latter is accounted for by the α_{beam} factor. We assume here black body stellar radiation model which yields for the CoRoT and the *Kepler* bandpasses and for F-G-K spectral-type stars, α_{beam} value between 0.8 and 1.2.

- The α_{ellip} factor represents the response of the stellar surface to the tidal effect induced by the companion, and to first order can be written (Morris 1985) as

$$\alpha_{\text{ellip}} \simeq 0.15 \frac{(15 + u)(1 + g)}{3 - u}, \quad (4)$$

where g is the stellar gravity darkening coefficient, whose expected range is 0.3–1.0, and u is the limb-darkening coefficient, whose range is 0–1 and is typically ≈ 0.6 for solar-like stars (see, for example, Mazeh 2008). Thus, we estimate, that for F-G-K spectral-type stars, α_{ellip} value is between 1.0 and 2.4.

Note that the expression for A_{ellip} includes an extra $\sin i$ factor, in addition to the one that appears in the $m_2 \sin i$ factor of Equation 2. This reflects the stronger dependence of the ellipsoidal modulation on the inclination angle. If we know well enough all the other factors of α_{ellip} and α_{beam} and we derive A_{ellip} and A_{beam} , we can, at least in principle, estimate both $m_2 \sin i$ and $\sin i$.

- In our simplistic approximation we include in the reflection modulation the thermal emission from the dayside of the companion, assuming both are modulated with the same phase (e.g., Snellen et al. 2009). This approximation does not model the small phase shift of the reflection modulation that can be present if the companion is not tidally locked, or if there is advection of heat away from the sub-stellar point, as shown by Knutson et al. (2007). The amplitude of the modulation of the reflected light alone is

$$A_{\text{refl}} = p_{\text{geo}} \left(\frac{r_2}{a} \right)^2 \sin i, \quad (5)$$

where p_{geo} is the geometrical albedo. Rowe et al. (2008) found quite small albedo, of 0.03, for HD 209458b, but recent study (Cowan & Agol 2010) suggested that exo-planets could have much larger albedo, up to 0.5. We therefore estimate, somewhat arbitrarily, the geometrical albedo coefficient by $p_{\text{geo}} = 0.1\alpha_{\text{refl}}$, and estimate that the value of α_{refl} can be between 0.2 and 5.

3 THE BEER ALGORITHM

3.1 Two-harmonic search

Before searching for small periodic effects in any stellar lightcurve, we have to prepare and clean the data. This is done in two stages. In the first one we remove jumps and outliers, and in the second stage we identify and subtract the long-term variation of the lightcurve with the discrete cosine transform (Ahmed et al. 1974), adopted to unevenly spaced data. This is done by subtracting from the data a linear model of all cosine functions with frequencies from zero to 0.1 d^{-1} , with frequency separation of $1/(2T)$, T being the total time span of the lightcurve (see details of our approach in Mazeh & Faigler 2010).

We then proceed to fit the data with a model that includes the ellipsoidal, beaming and reflection effects for every possible period, P_{orb} . The algorithm approximates each of the three effects by pure sine/cosine function, relative to phase zero taken at the time of conjunction — t_{conj} , when the small companion is in front of the stellar component of the system. This fiducial point replaces the time of transit — t_{tran} , used when modeling transiting planets and eclipsing binaries (e.g., Mazeh & Faigler 2010). The reflection and the beaming effects are approximated by cosine and sine functions, respectively, with the orbital period, and the ellipsoidal effect by a cosine function with half the orbital period. In this approximation we express the stellar flux modulation ΔF as a fraction of the averaged flux \bar{F} , and as a function of $\hat{t} \equiv t - t_{\text{conj}}$:

$$\frac{\Delta F_{\text{ellip}}(\hat{t})}{\bar{F}} = -A_{\text{ellip}} \cos\left(\frac{2\pi}{P_{\text{orb}}/2}\hat{t}\right), \quad (6)$$

$$\frac{\Delta F_{\text{beam}}(\hat{t})}{\bar{F}} = A_{\text{beam}} \sin\left(\frac{2\pi}{P_{\text{orb}}}\hat{t}\right), \quad (7)$$

$$\frac{\Delta F_{\text{refl}}(\hat{t})}{\bar{F}} = -A_{\text{refl}} \cos\left(\frac{2\pi}{P_{\text{orb}}}\hat{t}\right), \quad (8)$$

where the coefficients, A_{ellip} , A_{beam} and A_{refl} are all positive.

We note that contrary to the case of transiting planets, like CoRoT-3b, we do *not* know *a priori* the time of t_{conj} . The algorithm therefore fits the cleaned, detrended lightcurve with a linear five-parameter model, consisting of two frequencies:

$$\mathcal{M}(\bar{t}) = a_0 + a_{1c} \cos\left(\frac{2\pi}{P_{\text{orb}}}\bar{t}\right) + a_{1s} \sin\left(\frac{2\pi}{P_{\text{orb}}}\bar{t}\right) + a_{2c} \cos\left(\frac{2\pi}{P_{\text{orb}}/2}\bar{t}\right) + a_{2s} \sin\left(\frac{2\pi}{P_{\text{orb}}/2}\bar{t}\right), \quad (9)$$

where \bar{t} is the time relative to some arbitrary zero time. Since in this model the amplitudes are free to be either positive or negative, the usual bias of over-estimating a sinusoid's amplitude when fitting noisy data is not present.

As explained, we expect a_{2s} to be close to zero and a_{2c} to be negative relative to the time of conjunction, so after the fitting is done we find t_{conj} that results in $a_{2s} = 0$ and a_{2c} being negative. This time is when the first harmonic model

$$\mathcal{M}_2(\bar{t}) = a_{2c} \cos\left(\frac{2\pi}{P_{\text{orb}}/2}\bar{t}\right) + a_{2s} \sin\left(\frac{2\pi}{P_{\text{orb}}/2}\bar{t}\right) \quad (10)$$

has its minimum. We note that because \mathcal{M}_2 presents the first harmonic component of the model, it has two minima per period. The algorithm choice between the two minima is detailed below.

The algorithm then performs a new linear fit with a four-parameter model:

$$\mathcal{M}(\hat{t}) = \hat{a}_0 + \hat{a}_{1c} \cos\left(\frac{2\pi}{P_{\text{orb}}}\hat{t}\right) + \hat{a}_{1s} \sin\left(\frac{2\pi}{P_{\text{orb}}}\hat{t}\right) + \hat{a}_{2c} \cos\left(\frac{2\pi}{P_{\text{orb}}/2}\hat{t}\right), \quad (11)$$

which is our final model for that period.

3.2 A likelihood parameter

So far, the search performs a regular double-harmonic search (e.g., Shporer & Mazeh 2006), and therefore the fitting process could find any values for the three amplitudes. We now exercise our astrophysical expectations for the amplitudes and phases of the three effects, and assign to each period a likelihood factor which expresses how likely are the derived ratio between the amplitudes of the beaming and the ellipsoidal effects, and the phase difference between the beaming and the reflection effects.

If indeed the modulation, with its double harmonic components, is induced by a low-mass companion with negligible luminosity, we expect \hat{a}_{1s} to represent the beaming effect and therefore to be positive and \hat{a}_{1c} to represent the reflection effect and therefore be negative. The \hat{a}_{1c} coefficient is negative by our definition of t_{conj} .

The algorithm therefore distinguishes between two cases:

- The beaming and the reflection coefficients, \hat{a}_{1s} and \hat{a}_{1c} , respectively, have opposite signs. In this case the algorithm chooses (between the two options, see above) t_{conj} so that \hat{a}_{1s} is positive and \hat{a}_{1c} is negative.
- The beaming and the reflection coefficients, \hat{a}_{1s} and \hat{a}_{1c} , respectively, have the same sign. In such a case the algorithm chooses (between the two options, see above) t_{conj} such that the more significant coefficient has the correct sign. The other coefficient is then set to zero.

Our model is therefore composed of two or three components, depending on the relative

signs of the sine and cosine components of the fitting. Because we are looking for a system that displays *both* beaming and ellipsoidal modulations, we consider as our model goodness-of-fit parameter the r.m.s. of the smaller between these two fitted modulations. To scale the goodness-of-fit we divide the model r.m.s. by that of the residuals relative of the total model. This definition implies that a prominent peak in the periodogram indicates that *both* modulations, the ellipsoidal *and* the beaming ones, are significant at the specific peak period. This ratio, derived for every possible period, marks the first stage of our periodogram.

We now proceed to assign a likelihood factor to the model. Using Equations (1) & (2) we get for the ratio between the amplitudes of the ellipsoidal and the beaming effects:

$$\mathcal{R} \equiv \frac{A_{\text{ellip}}}{A_{\text{beam}}} = 5 \frac{\alpha_{\text{ellip}}}{\alpha_{\text{beam}}} \left(\frac{M_*}{M_\odot} \right)^{-4/3} \left(\frac{R_*}{R_\odot} \right)^3 \left(\frac{P_{\text{orb}}}{1 \text{ day}} \right)^{-5/3} \sin i. \quad (12)$$

We note that the amplitude ratio of the two effects depends only on parameters associated with the stellar properties of the primary star and the orbital period and inclination, and does not depend on the companion mass. As such, this ratio can serve as basis for comparing and validating the relevance of the detected amplitudes.

To do that, we distinguish between the *expected* ratio

$$\mathcal{R}_{\text{exp}} \equiv 5 \frac{\alpha_{\text{ellip}}}{\alpha_{\text{beam}}} \left(\frac{M_*}{M_\odot} \right)^{-4/3} \left(\frac{R_*}{R_\odot} \right)^3 \left(\frac{P_{\text{orb}}}{1 \text{ day}} \right)^{-5/3} \sin i, \quad (13)$$

and the *observed* ratio, $\mathcal{R}_{\text{obs}} \equiv |\hat{a}_{2c}|/|\hat{a}_{1s}|$. Obviously, \mathcal{R}_{obs} is not known exactly, but can be described by a probability distribution, $Pr_{\text{obs}}(\mathcal{R})$, which depends on the precision of the two derived amplitudes.

Furthermore, our expectation for \mathcal{R}_{exp} also does not have a single value, due to lack of precise knowledge of its factors. However, we can generate for every star and period a likelihood function $\mathcal{F}_{\text{exp}}(\mathcal{R})$, which assigns a likelihood value to a range of possible values of \mathcal{R} . This function reflects the random distribution of the inclination, together with our prior distributions of the mass and radius of the given star, and the prior likelihood, depending on the theory, of a range of values of α_{beam} and α_{ellip} . The function $\mathcal{F}_{\text{exp}}(\mathcal{R})$ thus, in essence, encompasses our expectations of the system, and serves as a prior, defined such that its maximum is unity and minimum is zero.

To demonstrate the situation we plot the two functions in Figure 1 for the *Kepler* star K06521917, derived for a period of 1.345 day. In this example, the most probable \mathcal{R}_{exp} value is 10.01, while $\mathcal{R}_{\text{obs}} = 1.4 \pm 0.14$. The likelihood in this case is quite small — 0.07.

For a given period, the value of the likelihood factor, defined as

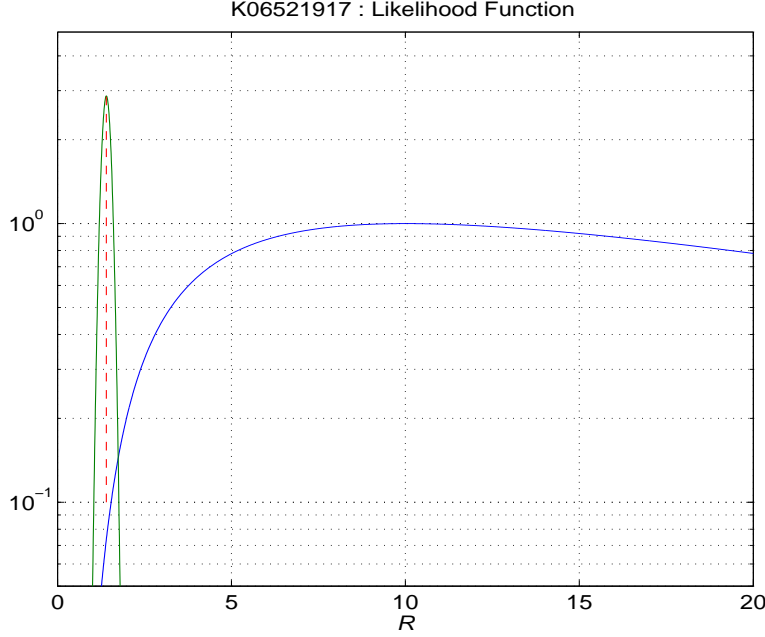


Figure 1. The likelihood function of the expected value of \mathcal{R}_{exp} (blue) and the probability distribution of the observed value of \mathcal{R}_{obs} (green) for the *Kepler* star K06521917, derived for a period of 1.345 day. The likelihood function peaks at $\mathcal{R} = 10.01$, and the probability distribution peaks at $\mathcal{R} = 1.4$, denoted by a vertical dashed line.

$$\mathcal{L}(P) = \int \mathcal{F}_{\text{exp}}(\mathcal{R}) \times Pr_{\text{obs}}(\mathcal{R}) d\mathcal{R}, \quad (14)$$

determines how likely are the two modulations to be caused by a low-mass companion for any given period. The likelihood factor is derived by integration over the probability distribution of \mathcal{R}_{obs} , weighted by the likelihood function. The final periodogram is the goodness-of-fit of the model multiplied by the likelihood factor $\mathcal{L}(P)$, generated for range of periods. The highest peak of each periodogram is our best estimate for the orbital period of the presumed low-mass companion.

3.3 Significance and detection limit

For any derived periodogram with its highest peak, we have to answer two questions:

- Is this peak significant, representing a real periodic modulation, or is it a result of random noise?
- If the peak is real and the stellar lightcurve does contain a periodic modulation, is this modulation induced by a low-mass companion?

The significance of a period detection can be estimated, for example, by the ratio of the highest peak to the second highest one in the periodogram, not including the harmonics of the highest peak. We choose to put our threshold detection when this ratio is 2. Bootstrap

simulations of 10,118 *Kepler* Q1 stars with magnitude within 12–13 range, and with radius smaller than $3R_{\odot}$, did not yield a single false detection using the factor 2 threshold, indicating a 99.99% significance. If a peak above this threshold is derived, we consider the corresponding star as a *candidate* host of low-mass companion, with the orbital period corresponding to the peak frequency.

Unfortunately, answering the second question is more difficult. Even with a highly significant peak at the periodogram, at this point we can not rule out false positive detections, which can rise from stellar modulations of some kind. Therefore, in order to confirm the detection of a low-mass companion, we do need follow-up RV observations. As the presumed period is known, a few measurements should be enough to confirm or reject the low-mass conjecture.

We now turn to roughly estimate our detection rate for the bright-star lightcurves of *Kepler*. To do that we took the actual Q1 lightcurves and added to them simulated beaming, ellipsoidal and reflection effects of binaries with a period of 3.2 days and randomly chosen phases. In this way, we used the real noise characteristics of the *Kepler* lightcurves to estimate the detection performance of the algorithm. The sample was composed of the 10,118 *Kepler* Q1 stars with magnitude within 12–13 range, and with radius smaller than $3R_{\odot}$, and the simulated effects were prepared with $\alpha_{\text{beam}} = 1$, $\alpha_{\text{ellip}} = 1.5$, $\alpha_{\text{refl}} = 1$, and $\sin i = \pi/4$, using the stellar masses and radii available from the *Kepler* catalog, all with the same secondary mass. We repeated the simulation for six different secondary masses — 10/20/40/80/160/320 M_{Jup} . In each simulation we applied the BEER algorithm and counted the stars for which the highest periodogram peak was at least twice as much higher than the next one, and we could detect both the beaming and the ellipsoidal modulations with 5σ significance. If the highest peak in our periodogram did not have the inserted period we did not consider that star as a detection.

The results are given in Figure 2, which indicates the fraction of systems that have been detected in the simulations as a function of the mass of the inserted modulation. We note that while the algorithm detected only one percent of the simulated massive planets, with masses of $10M_{\text{Jup}}$, almost all simulated modulations corresponding to a secondary mass of $\sim 0.3M_{\odot}$ were detected. The detection rate derived in this way indicates the potential of the BEER algorithm. We note that some of the non-detections may be caused by systems with *real* companions with different periods, with masses higher than the ones inserted by the simulation. This is specially true for the simulated $10M_{\text{Jup}}$ cases.

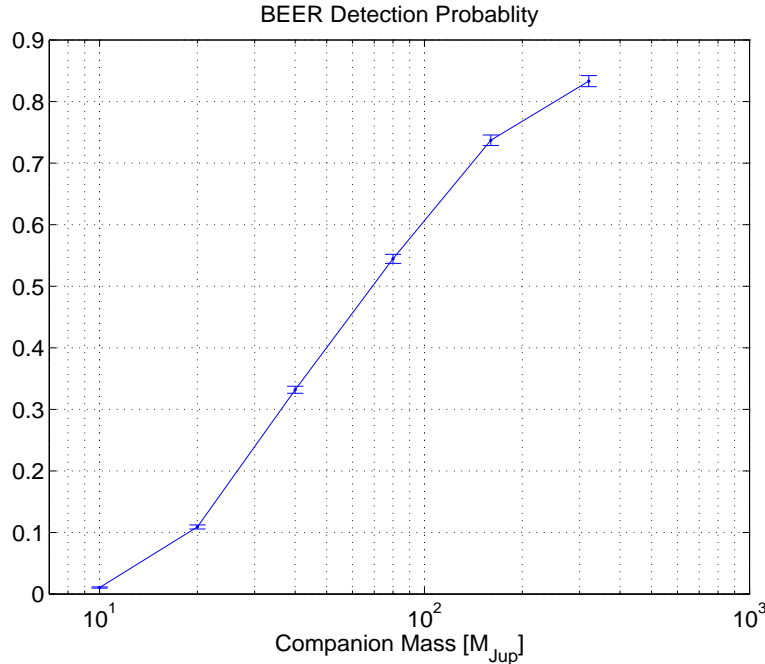


Figure 2. Percentage of 5σ detections of the BEER algorithm in our simulations, as a function of the secondary mass. Each of the simulations included a set of 10,118 *Kepler* Q1 stars, with magnitude within 12–13 range, and with radius smaller than $3R_{\odot}$ (see text).

4 TWO SIMPLE EXAMPLES

In order to demonstrate the effectiveness of the BEER algorithm, this section presents the detection of both the beaming and ellipsoidal modulations in two different *Kepler* lightcurves, induced by two low-mass companions. The two stars, KIC 08016222 (hereafter K6222) and KIC 010848064 (hereafter K8064), were found by the BEER algorithm, applied to the 11,249 brightest stars in the *Kepler* public lightcurves database (<http://archive.stsci.edu/kepler/>), with available stellar mass and radius estimate. In both lightcurves BEER detected periodic modulations, which we attributed in both cases to variations induced by a low-mass companion estimated, up to $\sin i$, at $\sim 70 M_{\text{Jup}}$. We chose to bring these two examples to demonstrate the precision of the *Kepler* mission, which allows detecting with high significance a companion with mass that could be in the lower end of the stellar mass range. In a separate paper (Faigler, Mazeh et al., in preparation) we present RV observations that confirm the existence of the two companions.

Figure 3 shows the obtained *Kepler* flux variation of the two stars, each of which is divided by its own mean flux. The lightcurves include only the Q1 released data, which lasted for 33 days, from May 13, 2009 until June 15, 2009.

In both lightcurves one can see a clear periodic modulation superposed on a long-term

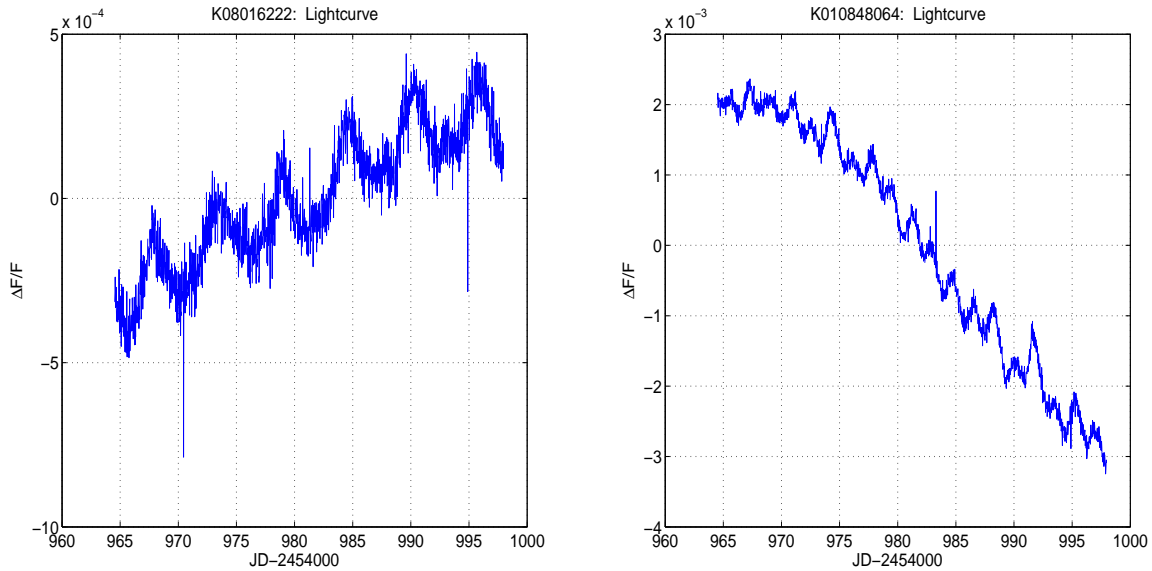


Figure 3. The original Q1 *Kepler* lightcurves of K6222 and K8064. The flux variation of each star is divided by its own mean. Left: K6222. Right: K8064. (Note the scale difference of the two panels).

variability of the stellar flux. Figure 4 shows the BEER periodograms of the two stars, using the cleaned detrended lightcurves (see Section 3.1). Both periodograms show a prominent peak, indicating the presence of a low-mass companion.

Figure 5 presents the likelihood function of the two stars for the best period found by the periodogram. The likelihood factor, based on Equation (14), is 0.99 and 0.97 for K8064 and K6222, respectively, implying that the detected periodic modulation *could* have been induced by a low-mass companion. Figure 6 presents the folded cleaned lightcurves, with phase zero defined to coincide with t_{conj} found by our algorithm for each star, together with the fitted BEER model.

Table 1 brings some details of the primaries of the two stars — estimated mass and radius and their *Kepler* magnitudes (<http://archive.stsci.edu/kepler/>), and presents the periods and derived amplitudes of the three effects found by the BEER algorithm for the two systems. It also brings the derived masses of the unseen companions, and the expected amplitude of the RV modulation.

One can see from Table 1 that the relative strength of the beaming and the ellipsoidal effects is quite different in the two stars. While for K8064 the derived amplitude of the ellipsoidal effect is larger than that of the beaming modulation, in the case of K6222, the derived beaming effect is almost three times larger than the ellipsoidal modulation. This difference changes the appearance of the folded lightcurves. This is so because the ellipsoidal effect is symmetric around phase 0.5, while the beaming effect is anti-symmetric. Therefore,

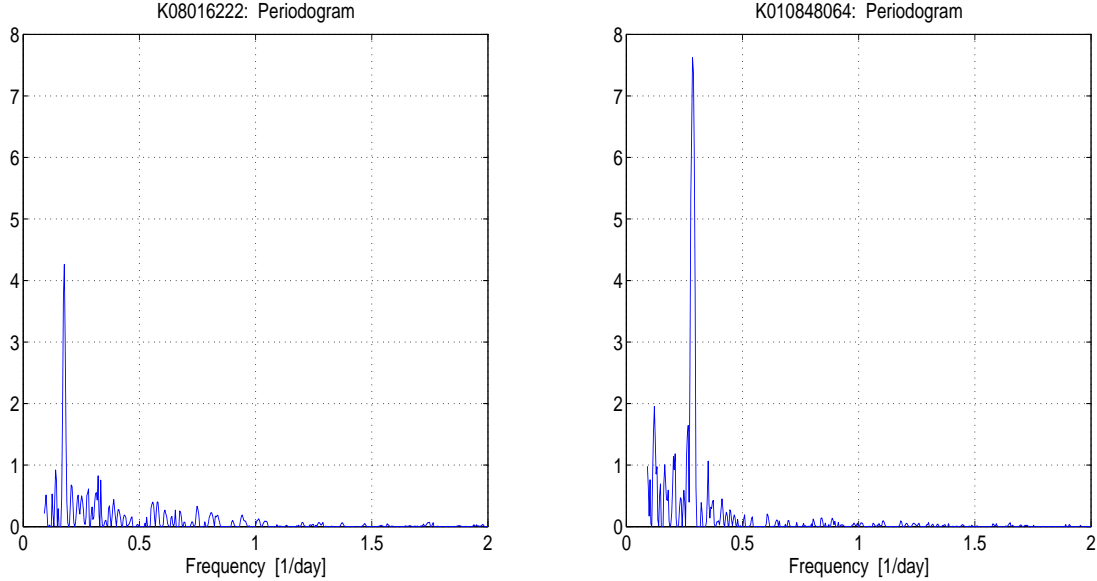


Figure 4. The derived periodograms of the BEER algorithm for the cleaned detrended lightcurves. Left: K6222. Right: K8064.

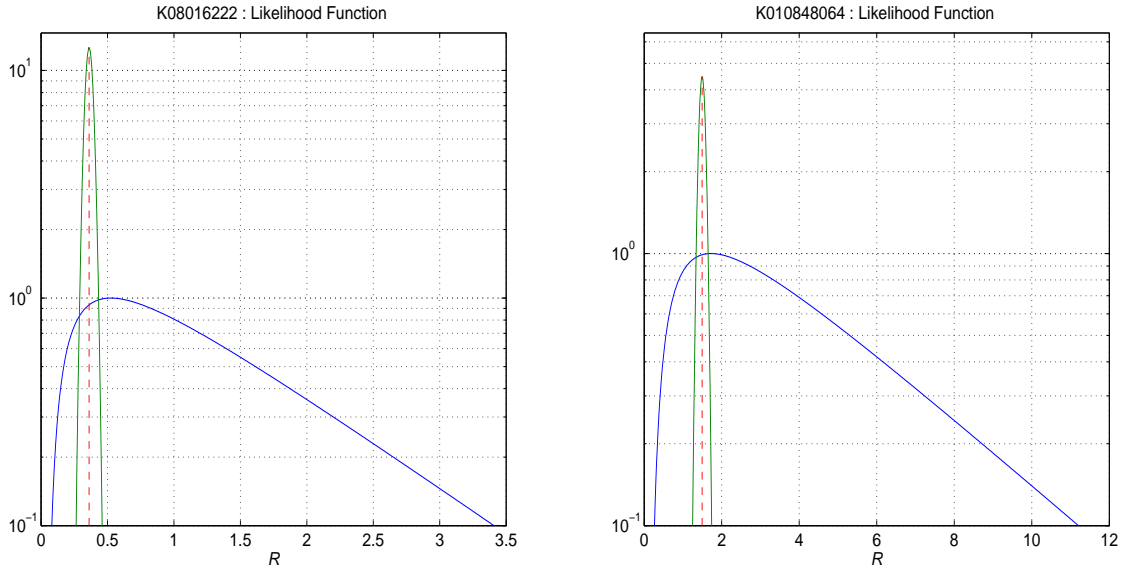


Figure 5. The likelihood function of the expected value of \mathcal{R}_{exp} (blue) and the probability distribution of the observed value of \mathcal{R}_{obs} (green), for the two examples. Left: K6222. Right: K8064. (Note the scale difference of the two panels).

the shape of the folded lightcurve of K8064 looks almost symmetric, while in the case of K6222 the symmetric appearance is completely lost.

The different ratio of the two amplitudes is rooted in Equation 12, which shows that this ratio depends on the stellar parameters of the primary, on the stellar radius to the third power in particular, and on the orbital period. As the *Kepler* estimate of the radius of K8064 is larger than that of K6222 and the derived orbital period is shorter, we expect the amplitude ratio of the two effects to be different for the two stars.

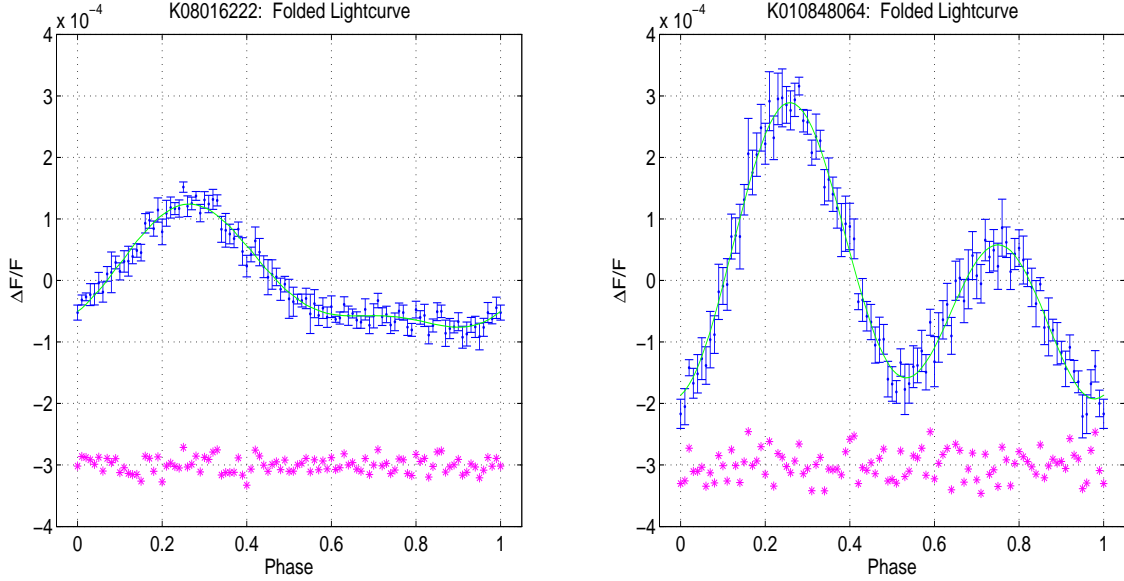


Figure 6. The folded cleaned lightcurves, binned into 100 bins, with the fitted model. The errors of each bin represent 1σ scatter of the measurements in each bin. The continuous line presents the BEER model. The residuals from this model are plotted at the bottom of the figure. Both panels have the same scale. Left: K6222. Right: K8064.

Table 1. The derived parameters of the three effects for K6222 & K8064

	K6222	K8064	
M_*	1.1	1.2	M_\odot
R_*	1.3	1.5	R_\odot
Kp	11.6	12.1	mag
Period	5.6 ± 0.2	3.53 ± 0.07	days
Ellipsoidal	34 ± 2	170 ± 5	ppm
Beaming	96 ± 2	116 ± 5	ppm
Reflection	11 ± 2	17 ± 5	ppm
$m_2 \sin i$	~ 70	~ 70	M_{Jup}
Expected K_{RV}	7	9	km/s

We opt not to give in this paper error estimates of the derived RV amplitudes and the inferred companion masses. Although the formal error of the RV amplitude can be derived from the error on the beaming amplitude, the true error is much larger, as we have to include the error coming from the inaccuracy of determining the orbital phase. This requires a further analysis that we defer to the paper which presents our analysis of all *Kepler* lightcurves (Faigler & Mazeh, in preparation). The companion mass error is even less known, as it depends not only of the amplitudes of the beaming and ellipsoidal effects, but also on the stellar primary mass, which is not well known at this stage. When we obtain spectra of the stars, we can better estimate the primary masses and give better constraints on the companion masses.

For both stars, the detection of the ellipsoidal and the beaming modulations was highly significant. The reflection effect, on the other hand, was less secure, as the amplitude of the

detected modulations was only 5 and 3 times their respective formal errors (see the discussion in the previous paragraph). However, as the two main effects were significantly detected, we estimated these detections as being secure, and considered these stars as candidates for hosting a low-mass companion. In a separate paper (Faigler, Mazeh et al., in preparation) we present RV observations that confirm the existence of the two low-mass companions, and demonstrate good agreement between the BEER predicted period and velocity amplitude, and the RV ones.

The analysis of K8064 & K6222 presented here was based on Q1 data only. After the BEER analysis *and* the performance of the RV observations that confirmed the photometric detection, the *Kepler* Q2 data was released. The Q2 lightcurves, with time span of additional 120 days, confirmed the detection of the photometric modulation. In particular, the newly derived photometric periods for both stars were consistent with the present photometric periods and the RV ones. The whole photometric data and RV measurements will be presented in the coming paper (Faigler, Mazeh et al., in preparation). Here we present only the Q1 data and analysis, to show how we actually discovered the two stars, in order to demonstrate the potential of the BEER algorithm.

5 DISCUSSION

We presented here a simple algorithm to detect candidates for low-mass *non-transiting* companions, using the *Kepler* and CoRoT lightcurves. The algorithm searches for the beaming effect, together with the ellipsoidal and the reflection modulations. The algorithm uses our prior knowledge of the stellar mass and radius, and the theory of tidal and beaming modulations, to verify that the ratio between the amplitudes of the beaming and ellipsoidal effects is as expected, and that the three effects have the correct relative phases. We expect the amplitudes of the effect to be on the order of 10–1000 ppm.

At the level of precision needed for this work, stellar activity will contaminate the signal, and worse yet, it will do so at a timescale that is comparable to the signals of interest, i.e. the orbital period. The associated flux modulations due to starspots can easily be larger than the expected beaming/ellipsoidal/reflection signal, and since the orbital period of the candidate is not known ahead of time, variations at the stellar rotation period can easily be of the correct duration to confound the BEER method. Therefore the BEER method can find only *candidates*, and RV observations are absolutely required for any confirmation. This

is similar to transiting searches, where RV follow-up measurements are crucial. To estimate statistically the yield of the BEER algorithm, the algorithm can be run on subsets of the data. RV follow up observations of the candidates found in the subsets can help determine the false alarm rate as a function of spectral type and magnitude.

The present version of the algorithm searches for a small-mass companion with a circular orbit. Obviously, an eccentric orbit will complicate the analysis, introducing higher harmonics of the orbital frequency. Radial-velocity modulation of eccentric orbit is a well understood effect, but the ellipsoidal modulation has still to be modeled carefully. Therefore, we assume in our analysis that the eccentricity contribution is small and defer more thorough analysis to the next stage of the development of the algorithm.

The two examples presented here demonstrated the potential of the *Kepler* lightcurves. The detection was done by using only the *Kepler* Q1 data, with timespan of only 33 days. We note that the detections were highly significant — the derived amplitudes of the beaming effect in both stars were on the order of 100 ppm, while the formal errors on the modulation amplitudes were 2 and 5 ppm for K6222 and K8064, respectively (but see the discussion in the previous section). If we ignore the stellar correlated noise (for its implication see, for example, Pont et al. 2006) we could expect the efficiency of the BEER algorithm to improve for longer lightcurves by up to \sqrt{n} , where n is the number of observations. Therefore, we can expect to be able to detect a periodic modulation with an amplitude of a few ppm when we will have access to more *Kepler* data, at least for stars with the same noise level as that of K6222 and K8064. Thus, it might be possible in the near future to find candidates for planets with mass as small as $5\text{--}10 M_{\text{Jup}}$. Mazeh & Faigler (2010) showed that the CoRoT data is also accurate enough to detect the beaming and the ellipsoidal effects induced by a brown-dwarf companion.

The long timespan of *Kepler* observations has one more advantage. If an analysis discovers an interesting candidate, follow-up RV measurements of this candidate can be obtained while the *Kepler* observations are still going on. This will enable the observer to compare not only the amplitude and period of the photometric beaming modulation with the RV observations, but also the phase of the detected beaming effect with the RV phase, confirming the existence of the low-mass companion with only very few RV observations. Furthermore, if enough RV measurements were obtained and independent RV phase can be established, comparing the phase of the follow-up RV observations with that of the ellipsoidal modulation can give us

some access to a possible lag between the two, which might indicate how the star is lagging after the tidal force exerted by its companion.

The attractiveness of the proposed approach is based on the fact that we have at hand on the order of a quarter of a million lightcurves (CoRoT and *Kepler* together) with precision high enough to detect low-mass companions, depending on the stellar brightness. It is almost equivalent of having an RV survey of many thousands of stars with precision of 1–5 km/s. This precision is enough to detect short-period low-mass-stellar, brown-dwarf companions, and even sometimes massive planets. Our simulations indicate that in the *Kepler* Q1 data we can detect about 30% of the brown-dwarfs with $40 M_{\text{Jup}}$ for stars with magnitude between 12 and 13 and stellar radii smaller than $3R_{\odot}$ (see Figure 2). We might expect that when we have at hand three years of *Kepler* data, with a timespan of ~ 1000 days instead of ~ 30 day, our detection threshold will improve by $\sim \sqrt{1000/30} \simeq 5$. This might be equivalent to have a modulation of $5 \times 40 M_{\text{Jup}}$ star in the present dataset. Consequently, we might expect that we will be able to detect 75% of the brown-dwarf secondaries of that sample. In upcoming papers (Faigler and Mazeh, in preparation) we list all the candidates found in the CoRoT and the *Kepler* data. These candidates, after confirmed, will increase the number of known low-mass-stellar/brown-dwarf companions and even massive planets.

The approach presented here could have been conceived only because of the vision of Loeb & Gaudi (2003) and Zucker et al. (2007), who anticipated such detections to happen well before the launch of CoRoT and *Kepler*. We feel deeply indebted to the authors of these two papers and to the teams of the CoRoT and *Kepler* satellites, who built and are maintaining these missions, enabling us to search and analyze their unprecedented photometric data.

ACKNOWLEDGEMENTS

We are indebted to Shay Zucker for helpful discussions and suggestions. We thank Dave Latham and Avi Shporer for careful reading of a previous version of the paper and illuminating comments. We thank to the anonymous referee whose comments and suggestions are highly appreciated.

All the photometric data presented in this paper were obtained from the Multimission Archive at the Space Telescope Science Institute (MAST). STScI is operated by the Association of Universities for Research in Astronomy, Inc., under NASA contract NAS5-26555.

Support for MAST for non-HST data is provided by the NASA Office of Space Science via grant NNX09AF08G and by other grants and contracts.

This research was supported by the ISRAEL SCIENCE FOUNDATION (grant No. 655/07).

REFERENCES

- Ahmed, N., T. Natarajan, T., & K. R. Rao, K.R. 1974, *IEEE Trans. Computers*, 90
- Aigrain, S., Favata, F., & Gilmore, G. 2004, *Astron. Astrophys.*, 414, 1139
- Auvergne, M., et al. 2009, *Astron. Astrophys.*, 506, 411
- Baglin, A., et al. 2006, 36th COSPAR Scientific Assembly, 36, 3749
- Borucki, W. J., et al. 2010, *Science*, 327, 977
- Carter, J. A., Rappaport, S., & Fabrycky, D. 2010, arXiv:1009.3271
- Cowan, N. B., & Agol, E. 2010, arXiv:1011.0428
- Deleuil, M., et al. 2008, *Astron. Astrophys.*, 491, 889
- Drake, A. J. 2003, *Ap. J.*, 589, 1020
- For, B.-Q., et al. 2010, *Ap. J.*, 708, 253
- Harrison, T. E., Howell, S. B., Huber, M. E., Osborne, H. L., Holtzman, J. A., Cash, J. L., & Gelino, D. M. 2003, *Astron. J.*, 125, 2609
- Knutson, et al. 2007, *Nature*, 447, 183
- Koch, D. G., et al. 2010, *Ap. J. Lett.*, 713, L79
- Loeb, A., & Gaudi, B. S. 2003, *Ap. J. Lett.*, 588, L117
- Maxted, P. F. L., Marsh, T. R., & North, R. C. 2000, *MNRAS*, 317, L41
- Maxted, P. F. L., Marsh, T. R., Heber, U., Morales-Rueda, L., North, R. C., & Lawson, W. A. 2002, *MNRAS*, 333, 231
- Mazeh, T. 2008, EAS Publications Series, 29, 1
- Mazeh, T., & Faigler, S. 2010, *Astron. Astrophys.*, 521, L59
- Morris, S. L. 1985, *Ap. J.*, 295, 143
- Pál, A., et al. 2008, *Ap. J.*, 680, 1450
- Pont, F., Zucker, S., & Queloz, D. 2006, *MNRAS*, 373, 231
- Reed, M. D., et al. 2010, *Astrophys. Space Sci.*, 329, 83
- Rouan, D., Baglin, A., Copet, E., Schneider, J., Barge, P., Deleuil, M., Vuillemin, A., & Léger, A. 1998, *Earth Moon and Planets*, 81, 79

- Rowe, J. F., et al. 2008, *Ap. J.*, 689, 1345
- Rowe, J. F., et al. 2010, *Ap. J. Lett.*, 713, L150
- Rybicki, G. B., & Lightman, A. P. 1979, *Radiative Processes in Astrophysics* (New York: Wiley)
- Shporer, A., & Mazeh, T. 2006, *MNRAS*, 370, 1429
- Snellen, I. A. G., de Mooij, E. J. W., & Albrecht, S. 2009, *Nature*, 459, 543
- van Kerkwijk, M. H., Rappaport, S. A., Breton, R. P., Justham, S., Podsiadlowski, P., & Han, Z. 2010, *Ap. J.*, 715, 51
- Welsh, W. F., Orosz, J. A., Seager, S., Fortney, J. J., Jenkins, J., Rowe, J. F., Koch, D., & Borucki, W. J. 2010, *Ap. J. Lett.*, 713, L145
- Zucker, S., Mazeh, T., & Alexander, T. 2007, *Ap. J.*, 670, 1326